Preferential Outward Diffusion of Ni in CuNi Alloy Proliferates Active Sites by An Order of Magnitude for OER and MOR

Roshini Arulraj[a], Tumpa Sadhukhan[a]*and Anantharaj Sengeni[b]*

[a]Theoretical and Computational Materials Chemistry Laboratory, Department of Chemistry, SRM Institute of Science and Technology, Kattankulathur 603203, Tamil Nadu, India

[b]Laboratory for Electrocatalysis and Energy, Department of Chemistry, Indian Institute of Technology, Kanpur 208 016, Uttar Pradesh, India

* Correspondence should be addressed to: tumpas@srmist.edu.in, and ananths@iitk.ac.in

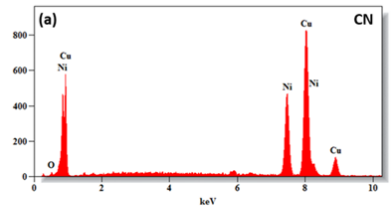

Element	Net Counts	Weight %	Atom %	Atom % Error	Formula
O	111	1.61	5.97	± 0.86	O
Ni	7662	30.02	30.30	± 0.69	Ni
Cu	14856	68.36	63.74	± 1.04	Cu
Total		100.00	100.00		

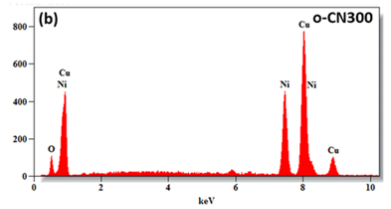

Element	Net Counts	Weight %	Atom %	Atom % Error	Formula
O	876	10.72	31.74	± 1.01	O
Ni	7983	28.35	22.87	± 0.55	Ni
Cu	14593	60.92	45.39	± 0.81	Cu
Total		100.00	100.00		

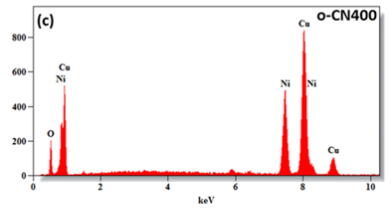

Element	Net Counts	Weight %	Atom %	Atom % Error	Formula
O	1129	13.33	37.31	± 1.26	O
Ni	7987	27.85	21.24	± 0.48	Ni
Cu	14350	58.82	41.45	± 0.70	Cu
Total		100.00	100.00		

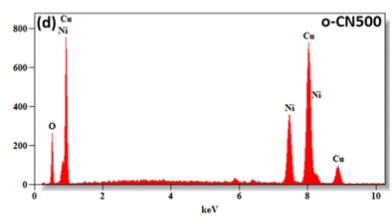

Element	Net Counts	Weight %	Atom %	Atom % Error	Formula
O	1408	18.35	46.61	± 1.26	O
Ni	5624	22.43	15.52	± 0.43	Ni
Cu	12624	59.22	37.86	± 0.67	Cu
Total		100.00	100.00		

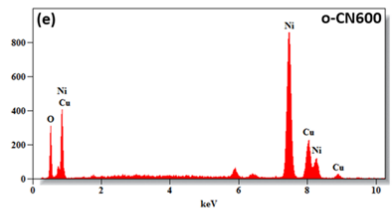

Element	Net Counts	Weight %	Atom %	Atom % Error	Formula
O	1642	20.05	48.38	± 1.30	O
Ni	14602	60.71	39.93	± 0.57	Ni
Cu	3933	19.25	11.69	± 0.52	Cu
Total		100.00	100.00		

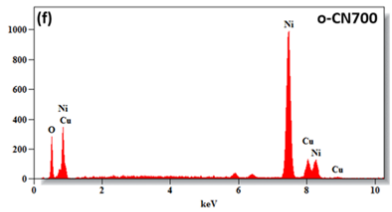

Element	Net Counts	Weight %	Atom %	Atom % Error	Formula
O	1535	18.97	46.45	± 1.24	O
Ni	16588	70.75	47.21	± 0.62	Ni
Cu	2049	10.29	6.34	± 0.48	Cu
Total		100.00	100.00		

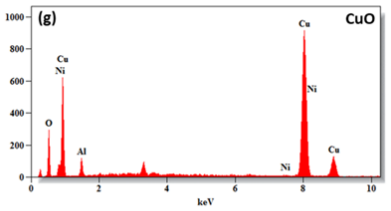

Element	Net Counts	Weight %	Atom %	Atom % Error	Formula
O	1597	21.19	49.25	± 1.30	O
Al	823	5.80	7.99	± 0.38	Al
Ni	161	0.63	0.40	± 0.09	Ni
Cu	15734	72.38	42.36	± 0.58	Cu
Total		100.00	100.00		

Figure S1: EDX spectra and corresponding elemental mapping of CN electrodes annealed at different temperatures: (a) pristine CN, (b) o-CN300, (c) o-CN400, (d) o-CN500, o-CN600, (e) o-CN700, and (g) peeled-off CuO. The maps show the distribution of Cu, Ni, and O, illustrating progressive surface oxidation with increasing annealing temperature.

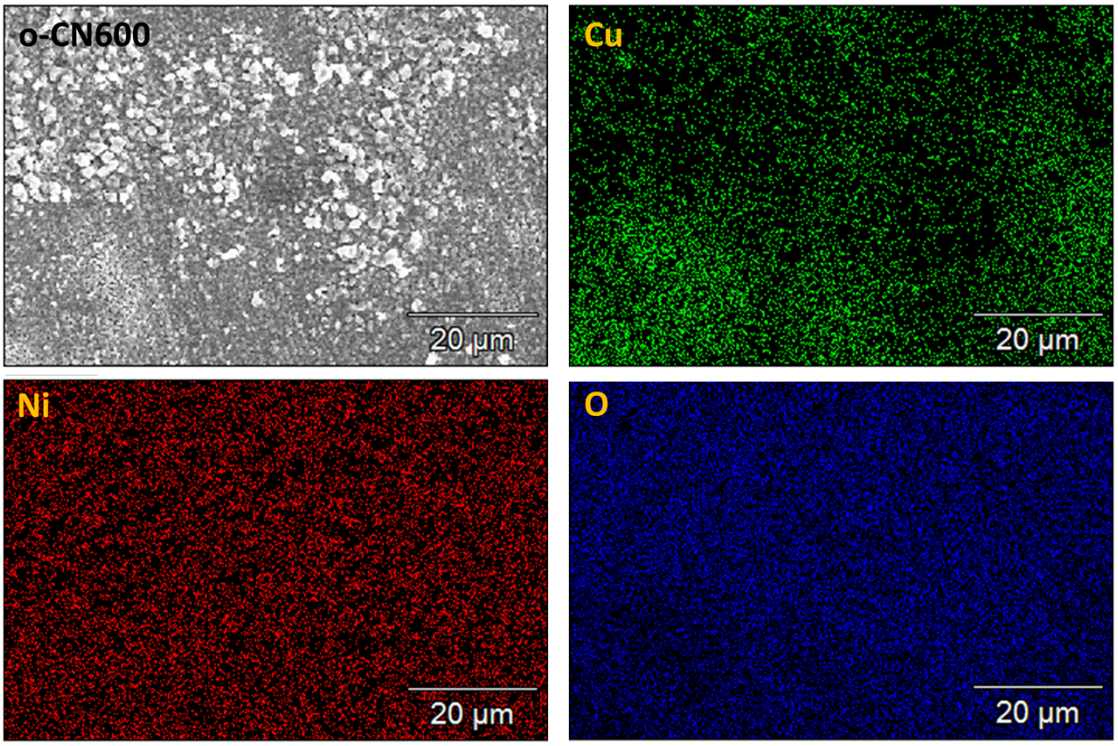

Figure S2: Elemental mapping of the CN electrode annealed at 600 °C (o-CN600), showing the distribution of Cu, Ni, and O.

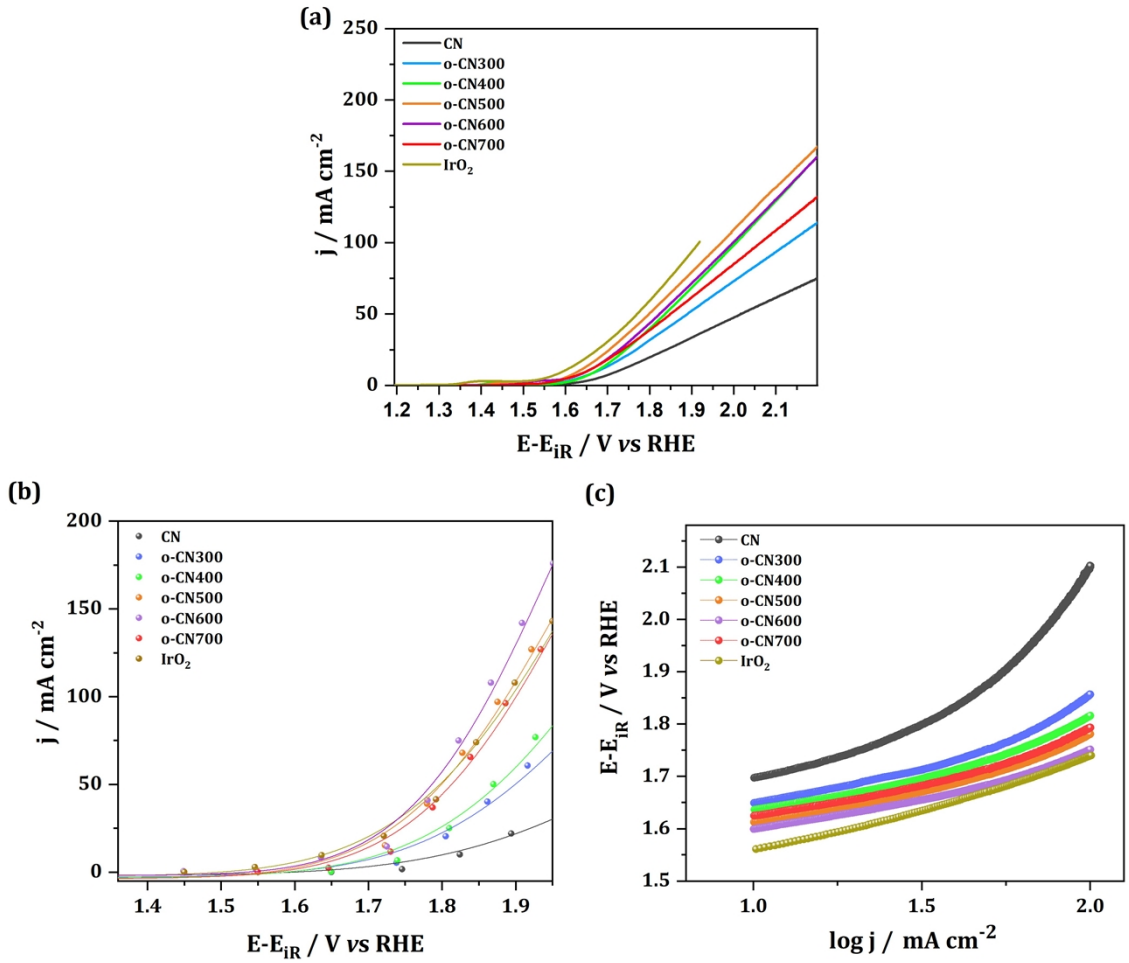

Figure S3: OER LSV curves of CN, o-CNX, and IrO_2/Ni without iR_u correction (a), SCV curves of CN and o-CNX (b), and corresponding Tafel plots derived from the LSV curves of CN and o-CNX (c).

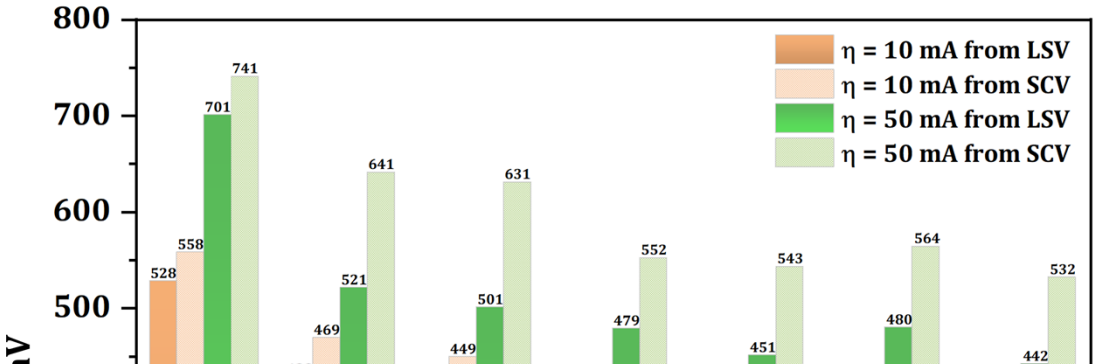

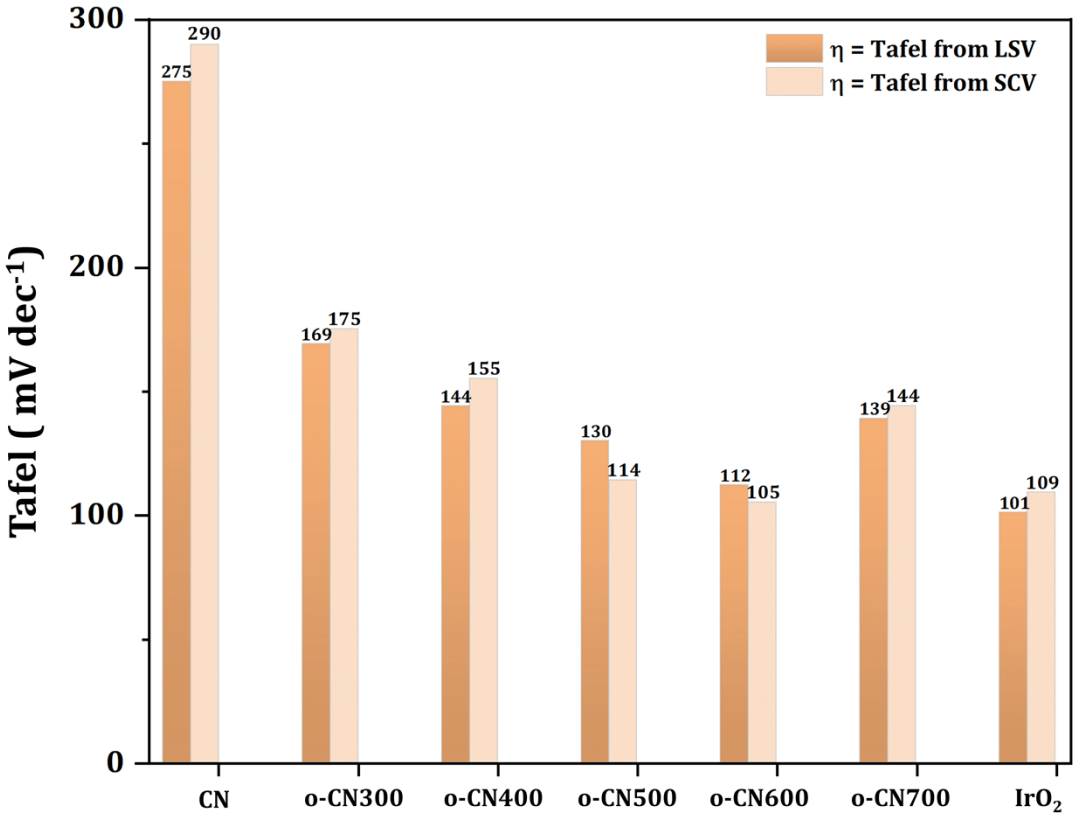

Figure S4: Overpotential comparison at 10 and 50 mA obtained from both LSV and SCV analyses.

Figure S5: Tafel comparison obtained from both LSV and SCV analyses.

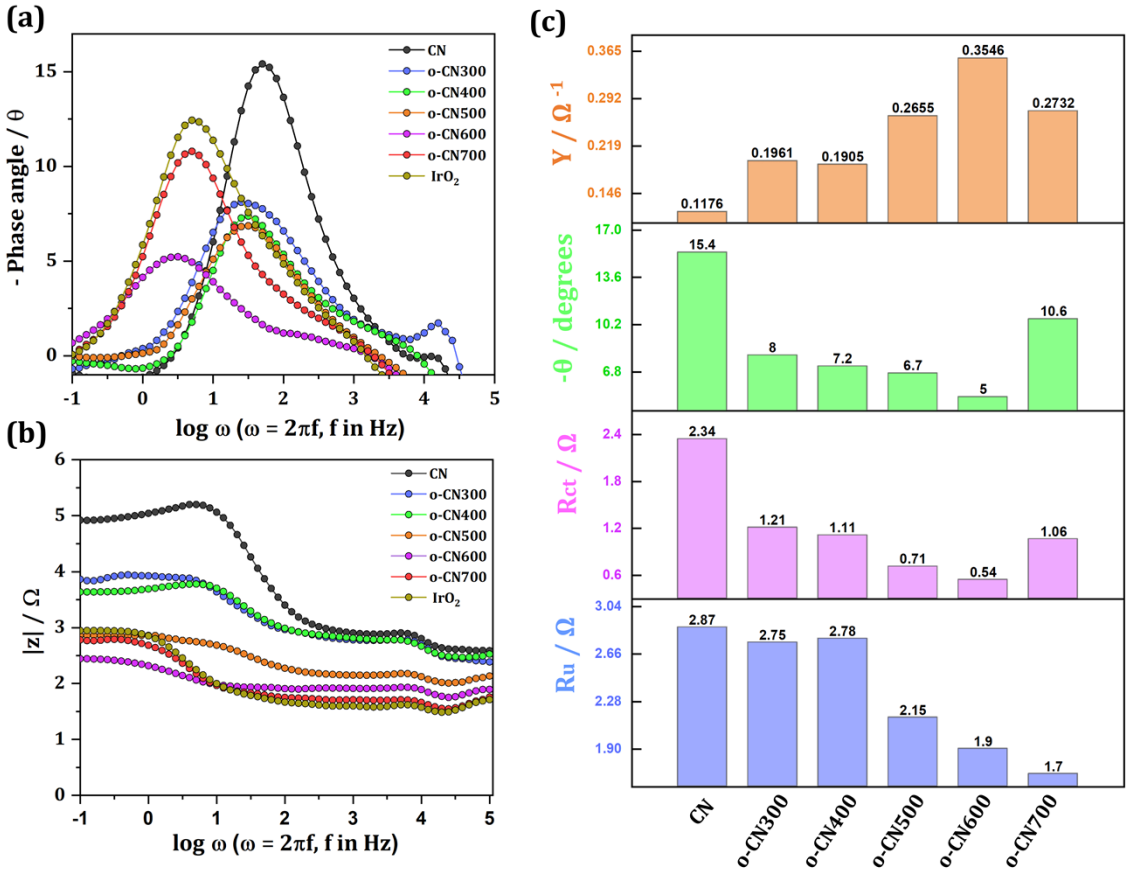

Figure S6: Bode phase-angle spectra (a); Bode magnitude plot showing the absolute impedance (b); and the corresponding EIS-derived parameters (c) for the CN and o-CNX during the OER process.

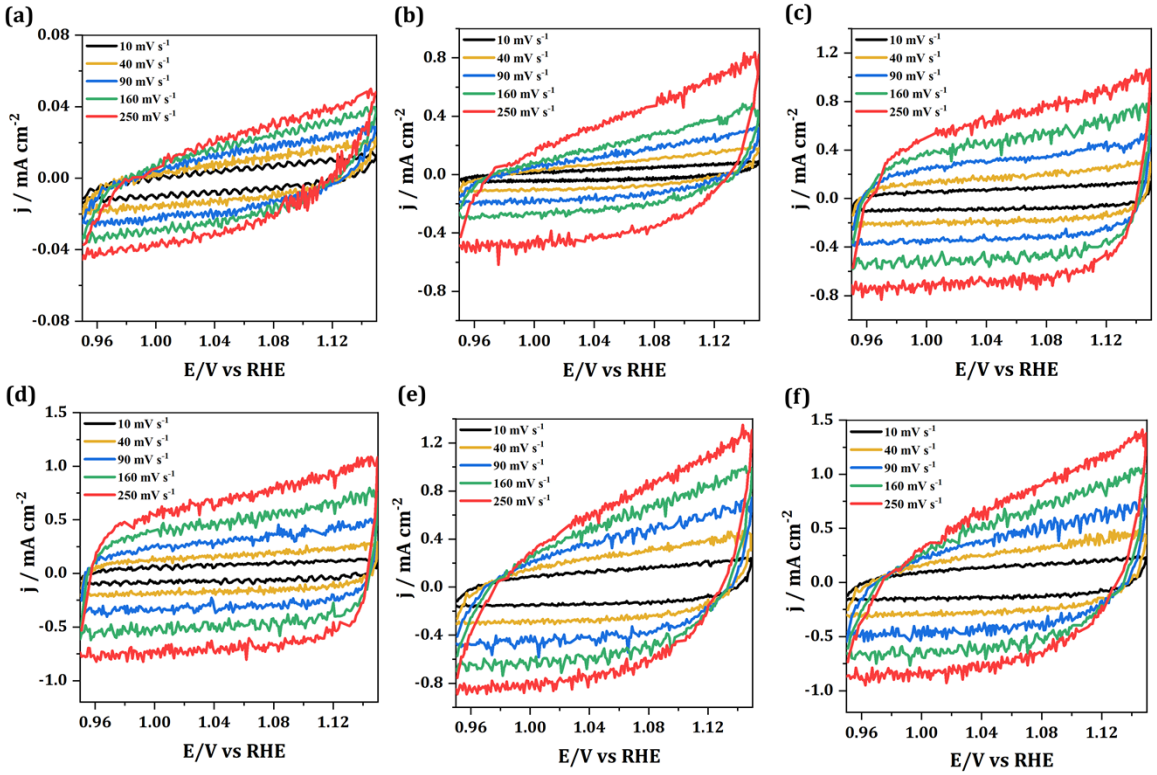

Figure S7: Panels (a–f) illustrate the electrochemical behavior within the non-Faradaic region of o-CNX.

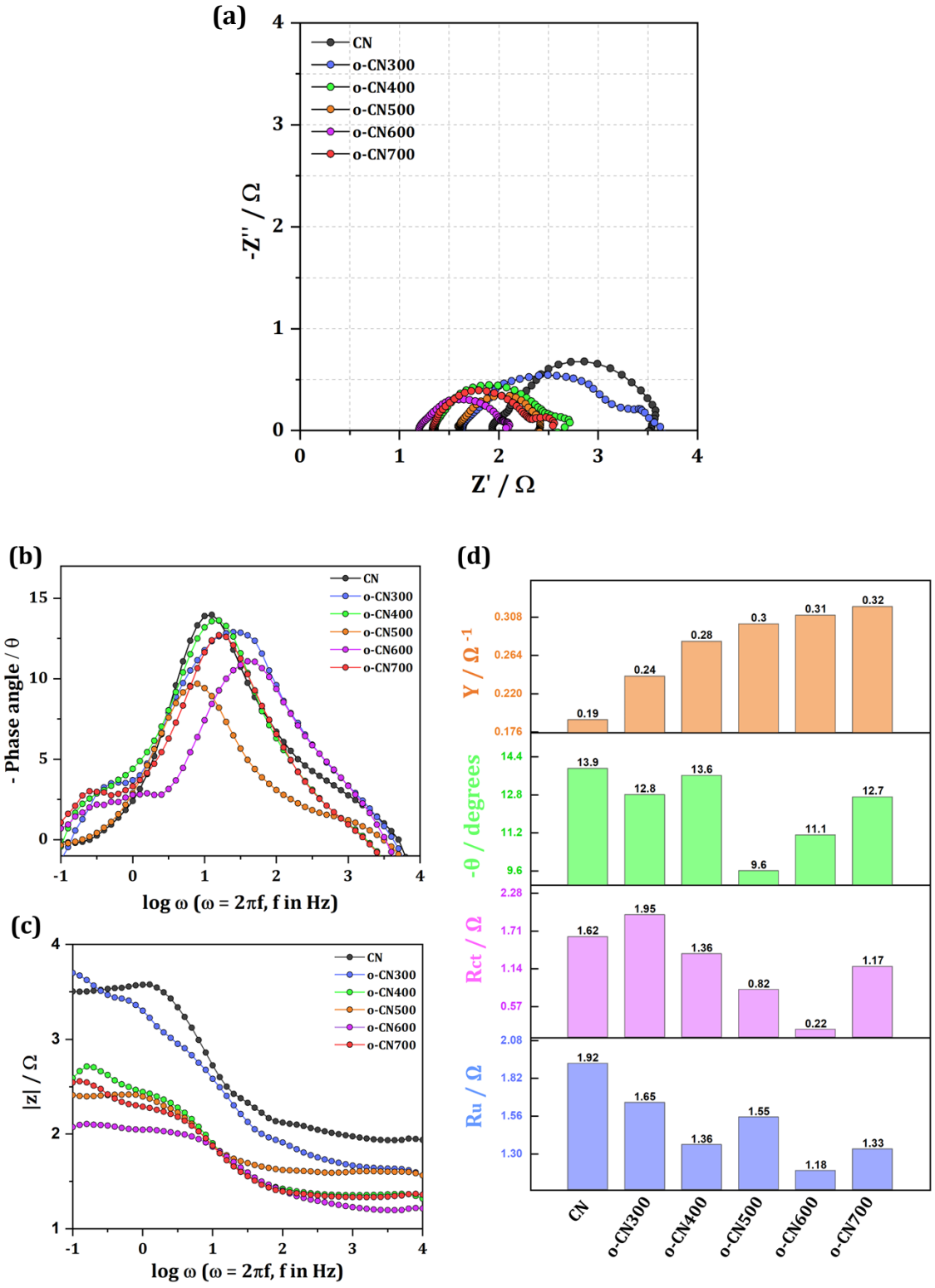

Figure S8: Nyquist plots for the CN and o-CNX series (a); Bode phase-angle plot (b); Bode magnitude plot showing the absolute impedance (c); and the corresponding EIS-derived parameters (d) for the CN and o-CNX during the MOR process.

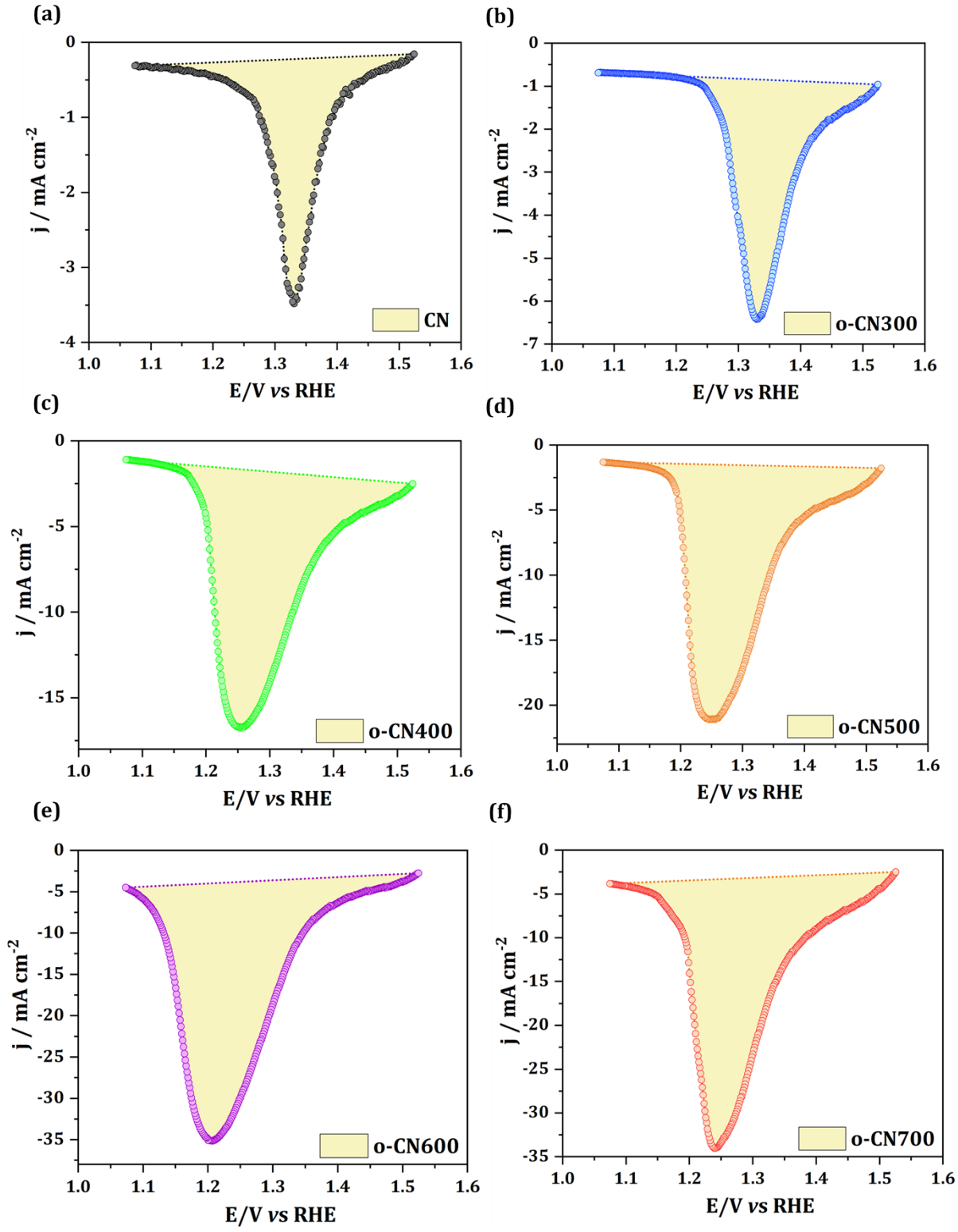

Figure S9: Backward CV scans collected for CN and o-CNX in 1.0 M KOH, serving as the basis for evaluating the ECAS (a–f).

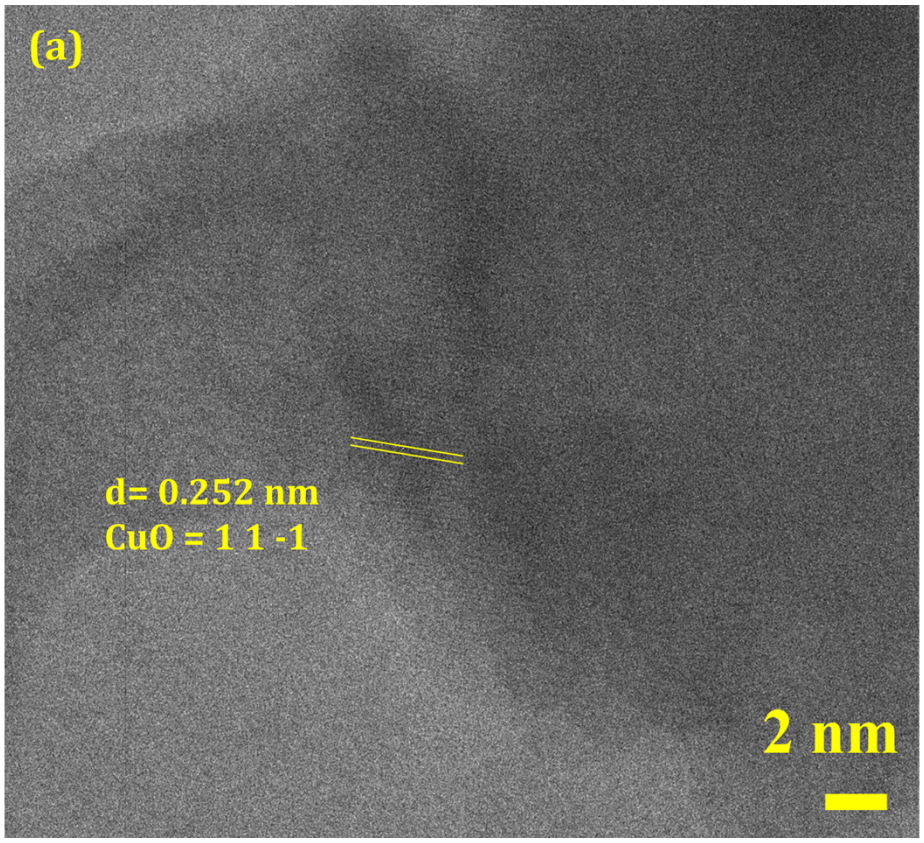
(a)
d= 0.252 nm
CuO = 1 1 -1
2 nm

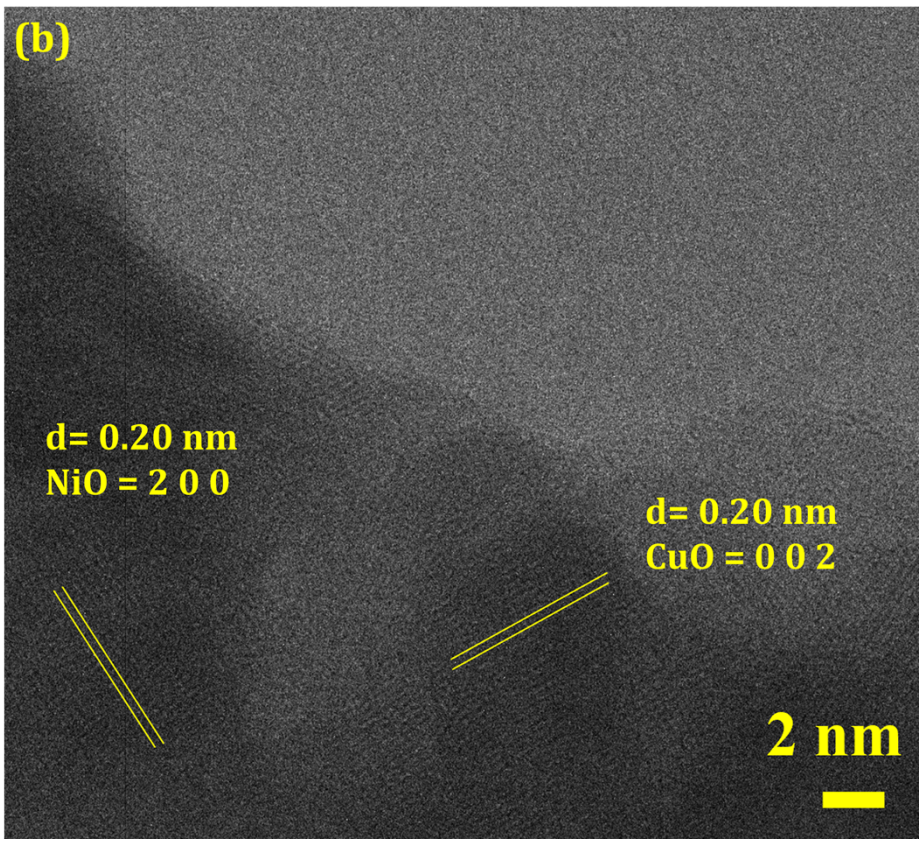
(b)
d= 0.20 nm
NiO = 2 0 0
d= 0.20 nm
CuO = 0 0 2
2 nm

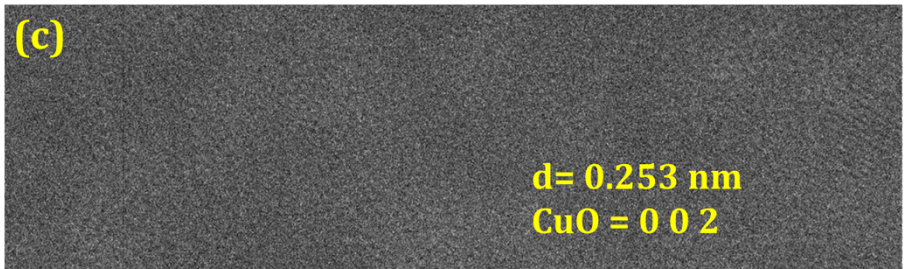
(c)
d= 0.253 nm
CuO = 0 0 2

Figure S10. High-resolution HRTEM images of the o-CN500, o-CN600, and o-CN700 samples shown in Figure 3. Panels are labeled in this figure as (a) - (c), corresponding to the main manuscript labels k, o, and s, respectively.

XPS Analysis and Mechanistic Insight:

Table S1. XPS-derived Ni^{2+}/Ni^{3+} ratios of the o-CN600 catalyst before and after the stability test

o-CN600	**Ni^{2+}/Ni^{3+}**	**$\%Ni^{2+}$**	**$\%Ni^{3+}$**
Before Stability	1.13	53.08	46.92
After Stability	1.83	64.59	35.41

Table S2. Comparison of the OER electrocatalytic performance of recently reported Cu–Ni-based catalysts and the present o-CN600 catalyst in alkaline electrolyte. The overpotential (η) values are compared at their corresponding current densities.

S. No.	**Catalyst**	**OER Overpotential (η)**	**Current Density ($mA\ cm^{-2}$)**
1	CuNiPx-GDY (1:1)[1]	178 mV	10 $mA\ cm^{-2}$
2	CuNiPd (CNP-3)[2]	256 mV	10 $mA\ cm^{-2}$
3	$(Co_{0.21}\ Ni_{0.25}Cu_{0.54})_3Se_2$[3]	272 mV	10 $mA\ cm^{-2}$
4	CuNi/CoFe LDH@NF[4]	268 mV	50 $mA\ cm^{-2}$
5	CuNi@NiFeCu[5]	285 mV	50 $mA\ cm^{-2}$
6	$Cu_{50}Ni_{50}$ NP[6]	318 mV	10 $mA\ cm^{-2}$
7	CuNi@Ni(ON)/CNTs-Gr[7]	410 mV	100 $mA\ cm^{-2}$
8	**o-CN600 (Present work)**	**372 mV**	**10 $mA\ cm^{-2}$**

REFERENCES

1. J. Gao, Y. Li, X. Yu and Y. Ma, *J. Colloid Interface Sci.*, 2022, **628**, 508–518.
2. M. A. Ehsan, S. Manzoor, S. A. Khan, A. S. Hakeem, M. Mansha, S. Ali and S. I. Allakhverdiev, *J. Ind. Eng. Chem.*, 2025, **146**, 421–430.
3. X. Cao, E. Johnson and M. Nath, *J. Mater. Chem. A*, 2019, **7**, 1646–1651.
4. D. Wang, Y. Chu, Y. Wu, M. Zhu, L. Pan, R. Li, Y. Chen, W. Wang, N. Mitsuzaki and Z. Chen, *J. Mater. Chem. A*, 2024, **12**, 33680–33688.
5. D. Cao, H. Xu and D. Cheng, *Appl. Catal. B*, 2021, **298**, 120600.
6. E. Gioria, S. Li, A. Mazheika, R. Naumann d'Alnoncourt, A. Thomas and F. Rosowski, *Angew. Chem. Int. Ed.*, 2023, **62**, e202217888.
7. D. T. Tran, V. H. Hoa, S. Prabhakaran, D. H. Kim, N. H. Kim and J. H. Lee, *Appl. Catal. B*, 2021, **294**, 120263.